Loading and characterization of a printed-circuit-board atomic ion trap

Kenneth R. Brown, Robert J. Clark, Jaroslaw Labaziewicz, Philip Richerme, David R. Leibrandt, and Isaac L. Chuang
Center for Ultracold Atoms, Research Laboratory of Electronics and Department of Physics, Massachusetts Institute of Technology, Cambridge, Massachusetts 02139, USA

(Received 29 June 2006; published 19 January 2007)

We demonstrate loading of $^{88}Sr^{+}$ ions into a 0.5-mm-scale printed circuit board surface-electrode ion trap. We then characterize the trap by measuring the secular frequencies and comparing them to a three-dimensional simulation of the trap, and by measuring the stray electric fields along two of the trap's principal axes. Cancelling these fields by applying additional voltages enables a hundredfold increase in the trap lifetime to greater than ten minutes at a vacuum of 10^{-9} torr.

DOI: 10.1103/PhysRevA.75.015401 PACS number(s): 33.80.Ps

Surface-electrode ion traps [1–4] offer significant potential for realizing complicated geometries needed for large-scale quantum computation [5]. Their advantages include greater ease of fabrication than three-dimensional (3D) layered planar traps [6–8] and the ability to integrate control electronics below the electrode surface [9].

Here, we present an atomic-surface-electrode ion trap realized as a printed circuit board (PCB). PCB traps have previously been demonstrated with charged microspheres at moderate vacuums [2] and we show that the same technology can be used to build atomic ion traps at UHV. Although the size scale of a PCB ion trap is not suitable for large-scale quantum computation, PCB traps can be constructed at a size scale similar to current ion-trap quantum-information experiments and may allow few-qubit ion traps to be readily realized. Additionally, the ease of fabrication allows for the rapid testing of new trap geometries and ion shuttling techniques.

In this Brief Report, we demonstrate the loading of strontium ions into a ~1-mm-scale PCB surface-electrode trap. Following the design of a traditional four-rod linear Paul trap system [15], the trap is mounted in a standard UHV chamber pumped down to $\sim 10^{-9}$ torr, loaded with $^{88}Sr^{+}$ by electron-impact ionization of neutral atoms from a resistive oven source, and driven by an externally mounted helical resonator. A controlled buffer gas environment of up to 10^{-4} torr of ultrapure helium may be provided though a sensitive leak valve, monitored with a Bayard-Alpert ion gauge.

Our surface-electrode ion trap has five electrodes [1,2]: one center electrode at ground, two at rf potential, and two segmented dc electrodes (Fig. 1). The electrodes are copper, deposited on a low-rf-loss substrate (Rogers 4350B), and fabricated by Hughes circuits following standard methods for microwave circuits. In the loading region, slots are milled between the rf and dc electrodes to prevent shorting due to strontium buildup. The inner surfaces are plated with copper to minimize trap potential distortion due to the accumulation of stray surface charges. The electrical connections are made to the trap by ultrasonically soldering Kapton-coated Cu wires to the pads using 80/20 Au/Sn solder.

We note that standard PCB fabrication techniques can generate traces on the order of 100 μm, producing a trap of similar size to other ion traps used for quantum information [3,4,6–8]. However, the minimum slot size commonly available is ≈500 μm, and in the case of our trap was 850 μm (Fig. 1). Choosing a standard slot size minimizes the amount of custom fabrication required. The only modification of the standard PCB is the polishing of the trap surface to a 1 μm finish to reduce laser scatter into the detector.

Ions are detected by laser-induced fluorescence of the main 422 nm $5S_{1/2} \rightarrow 5P_{1/2}$ transition of strontium [15], using either an electron-multiplying CCD camera (Princeton Instruments PhotonMax) or a photomultiplier tube (Hamamatsu H6780-04). A laser tuned to 1092 nm addresses the $5P_{1/2} \rightarrow 4D_{3/2}$ transition to prevent shelving from the P state to the metastable D state. The two external cavity laser-diode sources are optically locked to low finesse cavities [16]. Typical laser powers at the trap center are 1.2 mW at 1092 nm and 20–50 μW at 422 nm.

The first step for loading a surface-electrode trap is the determination of the ideal compensation voltages needed to offset the inherent electrode asymmetry. We determine these potentials numerically (using CPO, a boundary-element electrostatic solver [17]), by computing the rf and dc potentials

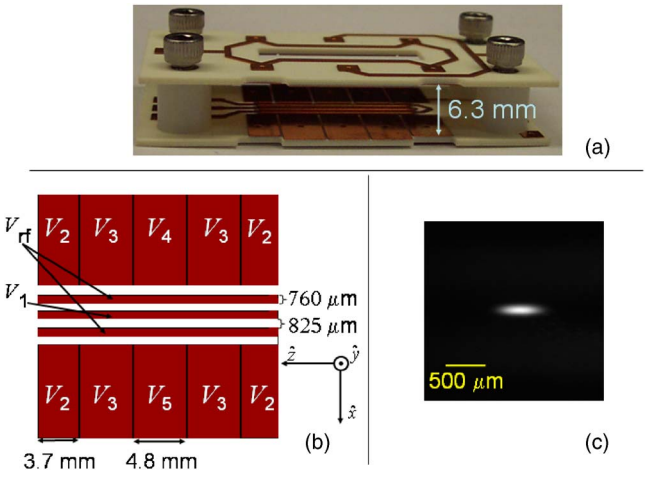

FIG. 1. (Color online) (a) Photograph showing the top electrode plate mounted 6.3 mm above the trap. The top plate has a slit for ion fluorescence detection. (b) Layout of trap electrodes, each labeled with the voltage applied; all but V_{rf} are dc. The space around the long electrodes (V_{rf} and V_1) has been milled out. Coordinates referenced as shown define the origin at the trap center and on the chip surface. (c) Charge-coupled device image of trapped strontium ions.

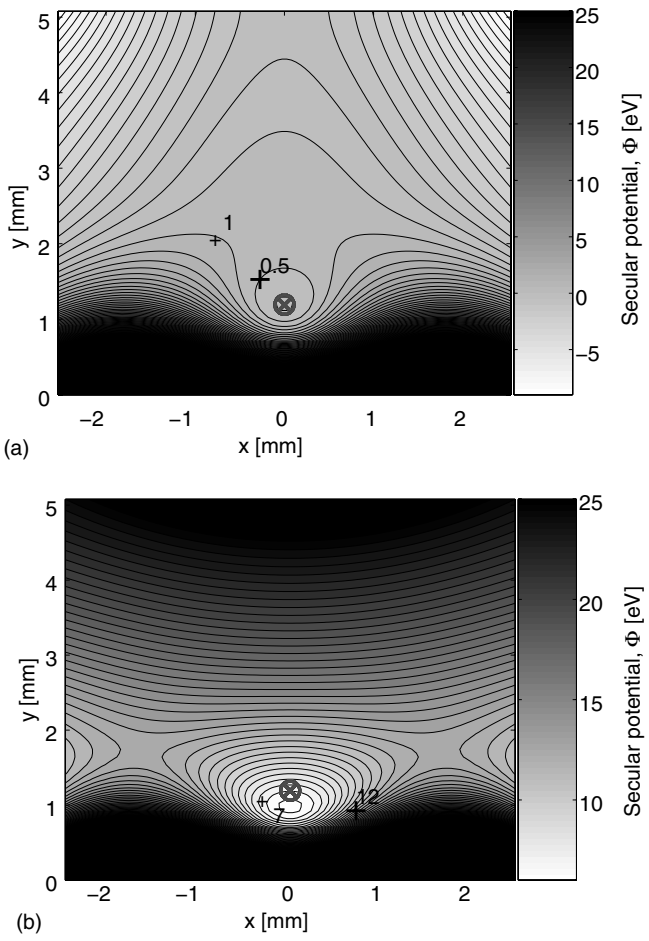

FIG. 2. Cross sections of the pseudopotential along the $\hat{x}$ and $\hat{y}$ directions for $V_{\mathrm{rf}}=1260$ V at $\Omega/2\pi=7.6$ MHz, $V_2=110$ V, and $V_3=-50$ V. The two figures (a) and (b) correspond to V_{top} voltages of −25.4 and 15 V, respectively. Micromotion compensation is expected in the −25.4 V case, but with a depth of only 1 eV, while the uncompensated 15 V case has an expected depth of 5.4 eV. The position of the rf null is indicated in each plot by an "⊗."

($\phi_{\mathrm{rf}}\cos\Omega t$ and ϕ_{dc}), which give the secular potential $\Phi=Q^2|\nabla\phi_{\mathrm{rf}}|^2/4m\Omega^2+Q\phi_{\mathrm{dc}}$, where m is the ion mass and Q is the ion charge. Typically, V_{rf} is of 500–1200 V amplitude at $\Omega/2\pi=7.6$ MHz, and dc electrode voltages (as defined in Fig. 1) are $V_4=V_5=0$ V, $V_2=110$ V, and $V_3=-50$ V.

Surface-electrode ion traps have a unique property compared to symmetric 3D Paul traps that the trap depth can be increased by applying a voltage V_{top} to the plate above the trap that moves the trap minimum away from the rf null. Although this increases micromotion, it can be a useful tool to increase loading efficiency. Shown in Fig. 2 is a cross section of the secular potential in the $\hat{x}$-$\hat{y}$ plane, at $z=0$, for two different values of V_{top}. As demonstrated in Fig. 3, with these voltages and $V_{\mathrm{top}}=-25.4$ V applied to the top electrode, the trap should be compensated with a trap depth of 1.0 eV. The trap depth can be increased to 5.4 eV by setting $V_{\mathrm{top}}=15$ V, at the cost of increased micromotion.

These ideal compensation voltages often differ substantially from actual ones, due to the presence of unknown stray charges in the trap [10–12]. By measuring the change in ion

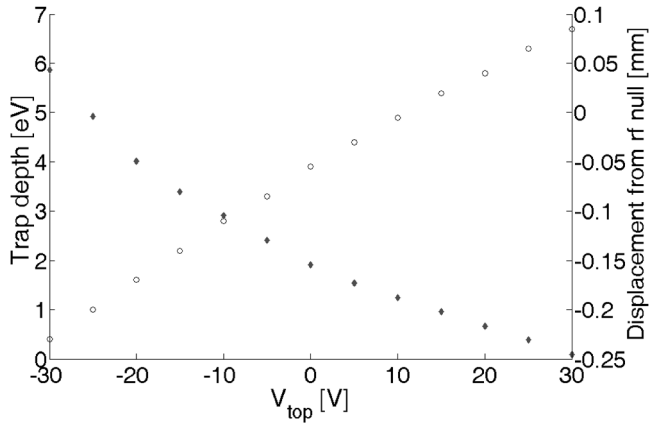

FIG. 3. Calculated values of trap depth (hollow circles) and ion displacement from the rf null (solid diamonds) as V_{top} is varied. As trap depth is increased, the displacement of the ion cloud from the rf null leads to increased micromotion.

cloud position with pseudopotential depth [10], the magnitude of the stray fields can be measured and the trap can be directly compensated.

An accurate value of the stray dc field can be calculated from the cloud motion using the following model. The electric field along a coordinate x, at the rf node, is well approximated by $E(x)=E_0+E_1x$. For an rf pseudopotential with secular frequency ω, the ion motion follows $m\ddot{x}+m\omega^2x+eE(x)=0$, which results in a new secular frequency $\omega_1=\sqrt{(\omega^2+eE_1/m)}$, and a new cloud center position $x_0=eE_0/m\omega_1^2$. By measuring both the secular frequency and the ion center, one can determine E_0.

We experimentally determine E_0 by measuring the cloud center position as a function of applied voltages. The 1092 nm laser is configured to illuminate the entire trapping region, while the 422 nm laser is focused to a 60 μm spot; the focal point is translated in the $\hat{x}$-$\hat{y}$ plane by using a precision motorized stage. Ion cloud fluorescence intensity, measured by the photomultiplier tube, is recorded as a function of laser position, and fit to a Gaussian centered at the ion cloud position [18]. This measurement is then repeated at ten different rf voltages, and a linear fit of the cloud center positions to $1/\omega_1^2$ determines the dc field value E_0. ω_1 is determined by applying an oscillating voltage on V_5 of 250 mV and observing dips in the ion fluorescence.

The data obtained, shown in Fig. 4, give an excellent match of the cloud intensity to a Gaussian fit, allowing measurement of the cloud center to within ±0.5 μm. Thus, the measurement of electric fields is precise to about ±10 V/m at zero electric field. From these electric-field measurements, we determine the required compensation voltages to be $V_{\mathrm{top}}=1.0\pm0.1$ V and $V_5=1.3\pm0.3$ V. The estimated residual displacement of a single ion at these voltages is less than 0.2 μm. A common feature of electron-impact ionization is that the compensation values change with time. We find that for this trap the values of V_{top} and V_5 change by ±1 V over ten loads. The nonlinear dependence of the dc electric field along $\hat{y}$ on the top electrode voltage is due to the strong anharmonicity of the trap in the vertical direction, unaccounted for in the simple linear model employed in the analysis.

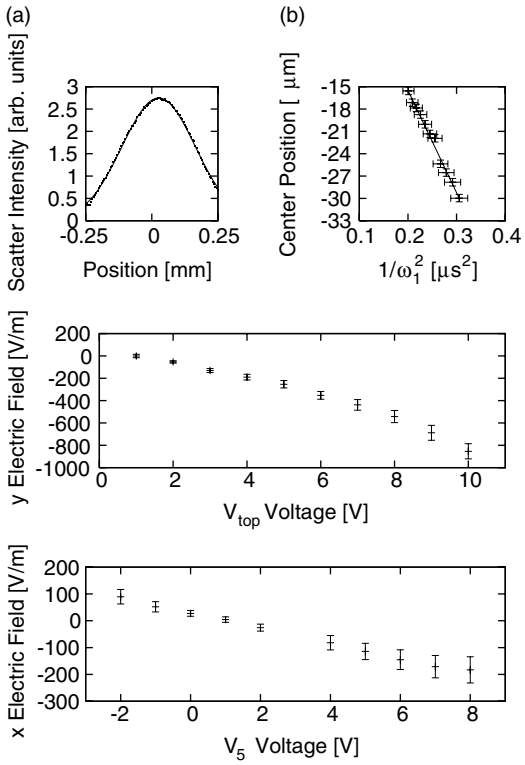

FIG. 4. Measurement results showing compensation of micromotion in the trap at a buffer gas pressure of 1×10^{-5} torr. (a) Cloud intensity profile along the $\hat{y}$ axis, fit to a Gaussian, for a representative value of the $\hat{y}$ compensation voltage, V_{top}. (b) Linear fit of the cloud center position versus $1/\omega_1^2$, where ω_1 is the secular frequency of the ion motion, yielding the electric field along $\hat{y}$ at the rf node. (c) Plot of the $\hat{y}$ electric field as a function of the V_{top} compensating voltage, showing that the stray field is minimized at $V_{\text{top}}=1.0$ V. (d) Plot of the $\hat{x}$ electric field as a function of the middle electrode voltage V_5, showing compensation at $V_5=1.3$ V.

At the ideal compensation voltages $V_5=0$ V and $V_{\text{top}}=-24.5$ V, the electric field should be zero. By measuring the actual electric field at these values, the magnitude of the stray field can be determined. At $V_5=0$ V and with $E_y=0$ ($V_{\text{top}}=1$ V), the stray field along $\hat{x}$ was measured to be 30 V/m. The trap was unstable for $V_{\text{top}}=-24.5$ V and the stray field was estimated by linear extrapolation to be $E_y\approx2000$ V/m from Fig. 4(c). This is in order-of-magnitude agreement with a parallel plate model, $E_y=(V_{\text{expt}}-V_{\text{ideal}}-V_1)/d=4200$ V/m, where V_{expt} is the experimentally determined compensation value ($V_{\text{top}}=1.0$ V), V_{ideal} is the ideal compensation value ($V_{\text{top}}=-24.5$ V), and d is the distance between the top plate and the trap ($d=6.3$ mm).

The secular frequencies differ from our model at the 5–10 % level, with greater differences along $\hat{y}$, presumably due to the larger $\hat{y}$ stray fields. For example, at one specific set of trapping voltages ($V_{\text{rf}}=950$ V, $V_1=V_4=V_5=0$ V, $V_2=V_3=20$ V, $V_{\text{top}}=10$ V), we measured secular frequencies of $\omega_x/2\pi=580$ kHz and $\omega_y/2\pi=840$ kHz. These deviate by 6 and 12%, respectively, from the predicted values of 543 and 742 kHz.

Also, as noted above, a stray field can rapidly reduce the trap depth. The abnormally large stray field required the use of the helium buffer gas in order to have sufficient signal and lifetimes to measure the field [13,14]. We used a helium pressure of 10^{-5} torr. The UHV lifetime in the absence of helium was less than 10 s. Once the field had been compensated, ion lifetimes at 10^{-9} torr were greater than ten minutes.

The pressure in this setup was limited by residual buffer-gas pressure and not the trap material. Rogers 4350B is made from FR4, which has been shown to have a low outgassing rate after bakeout [19]. We tested the vacuum properties of the PCB trap in a chamber with a 40 l/s ion pump and found that a pressure of 2×10^{-10} torr was obtained after five days of baking at 170 °C. This pressure is sufficient for few-qubit ion trap quantum information experiments.

The difference between measured and ideal compensation voltages is evidence of anisotropic stray fields, caused by undetermined surface charges. The estimated stray fields along $\hat{x}$ are comparable to those reported for 3D traps [10]. However, the stray fields along $\hat{y}$ are ten times larger. The 26 V difference between the calculated and measured values of V_{top} at compensation suggests significant electron charging on either the trap surface, the top plate, or the top observation window.

In summary, we have loaded a PCB surface-electrode ion trap, demonstrated that well-known compensation methods can be used in combination with collisional cooling to null even large stray fields, and measured pressure-limited trap lifetimes. PCB ion traps allow for the rapid prototyping and testing of different surface-electrode geometries, and may serve as a convenient architecture for studying ion motion in surface electrode traps and the loading of ions into microstructured trap arrays.

Support for this project was provided in part by the JST/CREST Urabe Project, and MURI project No. F49620-03-1-0420. We thank Rainer Blatt, Richart Slusher, Vladan Vuletic, and David Wineland for helpful discussions.

[1] J. Chiaverini, R. B. Blakestad, J. Britton, J. D. Jost, C. Langer, D. Leibfried, R. Ozeri, and D. J. Wineland, Quantum Inf. Comput. **5**, 419 (2005).

[2] C. E. Pearson, D. R. Leibrandt, W. S. Bakr, W. J. Mallard, K. R. Brown, and I. L. Chuang, Phys. Rev. A **73**, 032307 (2006).

[3] S. Seidelin, J. Chiaverini, R. Reichle, J. J. Bollinger, D. Leibfried, J. Britton, J. H. Wesenberg, R. B. Blakestad, R. J. Epstein, D. B. Hume, W. M. Itano, J. D. Jost, C. Langer, R. Ozeri, N. Shiga, and D. J. Wineland, Phys. Rev. Lett. **96**, 253003 (2006).

[4] J. Britton, D. Leibfried, J. Beall, R. B. Blakestad, J. J. Bollinger, J. Chiaverini, J. H. Wesenberg, R. J. Epstein, J. D. Jost,

D. Kielpinski, C. Langer, R. Ozeri, S. Seidelin, R. J. Reichle, N. Shiga, J. H. Wesenberg, and D. J. Wineland, e-print quant-ph/0605170.

[5] D. Kielpinski, C. Monroe, and D. J. Wineland, Nature (London) **417**, 709 (2002).

[6] M. D. Barrett, J. Chiaverini, T. Schaetz, J. Britton, W. M. Itano, J. D. Jost, E. Knill, D. Leibfried, C. Langer, R. Ozeri, and D. J. Wineland, Nature (London) **429**, 737 (2004).

[7] M. J. Madsen, W. K. Hensinger, D. Stick, J. A. Rabchuk, and C. Monroe, Appl. Phys. B: Lasers Opt. **78**, 639 (2004).

[8] D. Stick, W. K. Hensinger, S. Olmschenk, M. J. Madsen, K. Schwab, and C. Monroe, Nat. Phys. **2**, 36 (2006).

[9] J. Kim, S. Pau, Z. Ma, H. R. McLellan, J. V. Gates, A. Kornblit, R. E. Slusher, R. M. Jopson, I. Kang, and M. Dinu, Quantum Inf. Comput. **5**, 515 (2005).

[10] D. J. Berkeland, J. D. Miller, J. C. Bergquist, W. M. Itano, and D. J. Wineland, J. Appl. Phys. **83**, 5025 (1998).

[11] C. Raab, J. Eschner, J. Bolle, H. Oberst, F. Schmidt-Kaler, and R. Blatt, Phys. Rev. Lett. **85**, 538 (2000).

[12] C. Lisowski, M. Knoop, C. Champenois, G. Hagel, M. Vedel, and F. Vedel, Appl. Phys. B: Lasers Opt. **81**, 5 (2005).

[13] H. G. Dehmelt, Adv. At. Mol. Phys. **5**, 109 (1969).

[14] Y. Moriwaki, M. Tachikawa, Y. Maeno, and T. Shimizu, Jpn. J. Appl. Phys., Part 2 **31**, L1640 (1992).

[15] D. J. Berkeland, Rev. Sci. Instrum. **73**, 2856 (2002).

[16] K. Hayasaka, Opt. Commun. **206**, 401 (2002).

[17] B. Brkić, S. Taylor, J. F. Ralph, and N. France, Phys. Rev. A **73**, 012326 (2006).

[18] I. Siemers, R. Blatt, T. Sauter, and W. Neuhauser, Phys. Rev. A **38**, 5121 (1988).

[19] C. Rouki and L. Westerberg, and the CHICSi development group, Opt. Commun. **T104**, 107 (2003).